# Sequence Effects on Block Copolymer Self-Assembly through Tuning Chain Conformation and Segregation Strength Utilizing Sequence-Defined Polypeptoids

*Anastasia L. Patterson,[†] Scott P. O. Danielsen,[‡] Beihang Yu,[‡] Emily C. Davidson,[‡,§] Glenn H. Fredrickson,[†,‡,#] Rachel A. Segalman[†,‡,]**

[†]Materials Department, University of California, Santa Barbara, CA 93106

[‡]Department of Chemical Engineering, University of California, Santa Barbara, CA 93106

[#]Materials Research Laboratory, University of California, Santa Barbara, CA 93106

**For Table of Contents use only**

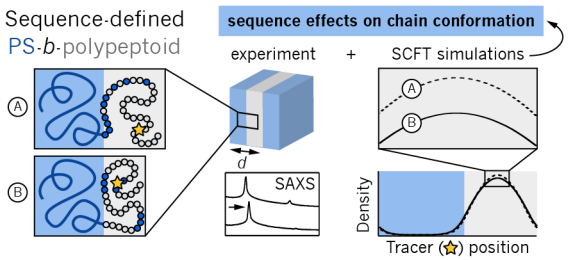

ABSTRACT

Polymers with sequence control offer the possibility of tuning segregation strength with comonomer sequence instead of chemical identity. Here, we have synthesized polystyrene-*b*-polypeptoid diblock copolymers that differ only in the sequence of comonomers in the polypeptoid block, where nonpolar phenyl side chains are incorporated to tune compatibility with polystyrene. Using small-angle X-ray scattering, we see that these materials readily self-assemble into lamellae, with domain spacings and order–disorder transition temperatures varying with sequence, despite identical composition. The ordered state is likely governed by chain conformational effects that localize compatibilizing comonomers at the block–block interface. These altered chain conformations are supported by simulations with self-consistent field theory (SCFT) and lead to the observed changes in domain spacing. However, the trends seen in the order–disorder transition are not captured by SCFT simulations or effective $\chi$ parameters, measured in the disordered phase by approximating the copolypeptoid as a uniform block. The disagreement between measured thermodynamic properties and coarse-grained approaches like SCFT and effective $\chi$ points to the importance of molecular-scale effects in sequence-defined materials. Additionally, a reversal in relative disordering temperatures between forward and inverse taper sequences is observed compared to previous studies, likely due to a combination of sequence definition at the monomer lengthscale and the use of a "styrene-like" compatibilizing side chain, rather than a true polystyrene repeat unit. These results demonstrate that comonomer sequence tunes chain conformation and segregation strength, suggesting that sequence design could be used to target desired properties and morphologies in block copolymer materials while retaining important chemical functionalities.

## INTRODUCTION

Block copolymers with tunable compatibility enable direct control over segregation strength, a key driving force for self-assembly and blend compatibilization. The segregation strength of a block copolymer ($\chi N$) can be tuned by changing the block–block interaction parameter ($\chi$), typically achieved by changing the chemical identity of one or both blocks, or the overall polymer size ($N$).[1] However, the $\chi$ parameter between blocks is difficult to predict, testing different materials can be synthetically impractical, and the choice of a particular chemistry or chain length is often integral to the function of the resulting material. With these restrictions, targeting and tuning block copolymer properties can be challenging.

One strategy toward tuning segregation strength is to incorporate compatibilizing groups into one or both blocks.[2,3] Experimental approaches have leveraged advances in controlled polymerization chemistries to produce smoothly-varying composition profiles that span the length of the chain (gradients), modify just the block junction (tapers), or insert comonomer-rich domains along the length of the chain, resulting in desirable morphologies and greatly reduced $T_{ODT}$s.[4-11] Further, molecular simulations have predicted that changing the sequence on the monomer lengthscale can affect dynamics, chain conformations, and morphologies, suggesting that synthetic control of not only composition profiles but comonomer sequence could lead to designing materials with predictable properties.[12-14] However, traditional synthetic approaches produce a disperse population of chains and cannot control the placement of single monomers, preventing experimental access to these precise sequences. Some synthetic strategies have been developed that target fine sequence control (often through sequence-defined macromonomers or iterative orthogonal reactions), and biopolymers such as polypeptides and nucleic acids are inherently sequence-defined, but until very recently, most of these approaches have either been

limited in production scale for use in bulk polymer physics studies or are not able to access arbitrary sequences.[15-23] There is considerable opportunity to experimentally investigate the range of promising behaviors expected for these precise materials.

Synthesized at large scale via highly efficient solid-phase synthesis,[24] polypeptoids (*N*-substituted polyglycines) are emerging materials for polymer applications where sequence plays a critical role in function. The exact sequence control afforded with this model system has led to discoveries in foldamers and self-assembling nanostructures in solution, and in bulk studies of crystallization and self-assembling systems for ion transport.[25-31] Pure polypeptoid and polystyrene–polypeptoid diblock copolymers have been shown to self-assemble into a variety of bulk microstructures.[32-36] In the study of polystyrene–polypeptoid materials, phenyl side chains incorporated into the polar polypeptoid block acted as compatibilizing groups, lowering the order–disorder transition temperature in a similar manner to gradient and taper copolymers.[36] With behavior resembling that of traditional polymer systems and unique synthetic control, polypeptoids are poised for studying precise compositional and sequence effects.

The present study demonstrates the ability for sequence control of comonomers to directly tune both the chain conformations and segregation strength of self-assembling block copolymers, resulting in differences in domain spacing and phase stability. Sequences with compatibilizing groups distributed along the chain length are observed to have smaller domain spacings and lower order–disorder transition temperatures than tapered sequences, likely due to chain conformations made possible by localization of compatibilizing groups at the microdomain interface. These conclusions are supported by simulations performed with self-consistent field theory (SCFT). The order–disorder transition temperature ($T_{ODT}$) is also observed to be a function of sequence, but the trend in $T_{ODT}$s does not match that seen with SCFT or effective

interaction parameters (extracted from scattering measurements in the disordered melt). We conclude that sequence-dependent chain conformations dominate the observed geometric and thermodynamic properties, and that coarse-grained approaches do not capture the molecular-scale physics at play in sequence-defined materials.

## EXPERIMENTAL AND THEORETICAL METHODS

### Materials

Solvents and reagents were purchased from commercial suppliers and used without further purification unless otherwise noted. Rink amide MBHA resin was purchased from Novabiochem at 0.78 mmol/g loading. Anhydrous dimethylformamide (DMF) and diisopropylethylamine (DIPEA) were used in click reactions. HPLC-grade tetrahydrofuran (THF), water, and acetonitrile were used for precipitations, lyophilization, and MALDI-MS sample preparation. Styrene, ethyl-α-bromoisobutyrate (EBiB), and *N,N,N′,N″,N″*-pentamethyldiethyltriamine (PMDETA) were filtered through alumina immediately before use.

### Synthesis of alkyne-terminated polypeptoids

Polypeptoids were synthesized as previously described.[24] First, rink amide resin (0.78 mmol/g, 300 μmol scale) was deprotected twice with 4-methylpiperidine (30 eq, 20% v/v in DMF). Bromoacetic acid (12 eq, 0.6 M in DMF) and diisopropylcarbodiimide (DIC, 11.5 eq, 59% v/v in DMF) were added and mixed for 20 min. The bromide chain end was then displaced with an amine (methoxyethylamine (Nme), phenylethylamine (Npe), or phenylpropylamine (Npp), 16 eq, 1M in DMF) for 1 hr. The resin was washed with DMF five times between each synthetic step. After the desired sequence was synthesized, an additional unit was added in the same

method, displacing with propargylamine (Nprg) to add an alkyne endgroup. Finally, the chain end was acetylated with a solution of equimolar acetic anhydride and pyridine (8 eq, 0.4 M in DMF), washed with DMF and dichloromethane (DCM), and dried with nitrogen flow. Polypeptoids were cleaved from the resin using 40 mL of a trifluoroacetic acid (TFA) cleavage cocktail with the composition DCM:TFA:$H_2O$ (48.75 : 48.75 : 2.5) for 10 min. The resin was filtered and rinsed with more cleavage cocktail and DCM. The collected solution was dried *in vacuo* and lyophilized twice from acetonitrile:water (1:1) solutions to yield white powders. *Note: TFA is a volatile strong acid. Evaporation was performed with a cold trap at –90 °C. Precautions were taken to isolate TFA waste streams.* Polypeptoid molecular weight was confirmed by MALDI-MS and UPLC-MS.

**Synthesis of azide-terminated polystyrene**

First, bromine-terminated polystyrene (PS) was synthesized via atom transfer radical polymerization (ATRP). EBiB (146 μL, 1 eq), PMDETA (42 μL, 0.2 eq), and styrene (5 g, 48 eq) were combined in an oven-dried Schlenk flask. The solution was sparged with nitrogen for 30 min before adding copper (I) bromide (29 mg, 0.2 eq). The mixture was further degassed with three freeze–pump–thaw cycles (to pressures <100 mTorr), and then stirred under a nitrogen atmosphere at 100 °C until the mixture solidified, approximately 24 hours. The solid was dissolved in THF, filtered through alumina to remove copper compounds, and then precipitated into 1 L methanol. The filtered polymer was dried in vacuo overnight at 35 °C before being redissolved in DMF (at 200 mg/mL) and combined with sodium azide (90 mg, 1.5 eq). The reaction was stirred overnight at room temperature, then precipitated twice into 1 L methanol, stirring the second precipitation overnight to fully separate trace sodium azide. *Note: Sodium*

*azide forms toxic and explosive hydrazoic acid when in contact with strong acids. Precautions were taken to isolate azide waste streams.* The final polymer was filtered and dried overnight *in vacuo* at 35 °C to yield a white solid. Molecular weight was determined by GPC against PS standards to be $M_n$ = 5200 g/mol, Đ = 1.12.

**Synthesis of polystyrene–polypeptoid diblock copolymers**

In a typical reaction, alkyne-terminated polypeptoid (100 mg) was combined with azide-terminated polystyrene (220 mg, 2 eq) and anhydrous DMF (3 mL) in an oven-dried flask. DIPEA (37 μL, 10 eq) and PMDETA (22 μL, 5 eq) were added, and the solution was sparged with nitrogen for 30 min. In a separate, oven-dried Schlenk flask, ascorbic acid (19 mg, 6 eq) and copper (I) bromide (15 mg, 5 eq) were added, and the flask was evacuated and backfilled with nitrogen three times. The sparged solution was added to the Schlenk flask with a degassed syringe, and the mixture was further degassed with three freeze–pump–thaw cycles (to pressures <100 mTorr), before stirring under static vacuum at 50 °C for 40 hours. The solution was then diluted with DMF and filtered through alumina to remove copper compounds. The filtrate was concentrated *in vacuo* and precipitated from THF into a mixture of 2:3 cyclohexane:hexanes to remove excess polystyrene. The precipitate was dried *in vacuo* before purifying by preparatory GPC with THF as the eluent. A final precipitation of the isolated product in 2:3 cyclohexane:hexanes and drying *in vacuo* yielded a clear, glassy solid. Purified block copolymer was characterized by MALDI-MS to ensure block coupling and the absence of unreacted homopolymer.

**Matrix-assisted laser desorption ionization mass spectrometry (MALDI-MS)**

MALDI-MS was performed on a Bruker Microflex LRF MALDI TOF mass spectrometer. All solutions were prepared in HPLC-quality THF. Samples were dissolved at 200 μM and combined 1:1 with 10 mg/mL dithranol (polypeptoids) or 20 mg/mL *trans*-2-[3-(4-*tert*-butylphenyl)-2-methyl-2-propenylidene]malonitrile (DCTB) with AgTFA added at 0.1 mg/mL to aid in ionization of polystyrene-containing materials. All matrix–sample mixtures were spotted (1 μL) onto a polished steel MALDI target plate (Bruker). Mass spectra were collected in positive reflectron (polypeptoids) or linear mode (diblocks copolymers), summing at least 600 shots. Mass peaks were calibrated against peptide and protein standards (Bruker, prepared as prescribed) in a mass range of 600–18,000 Da.

**Ultra-high-pressure liquid chromatography mass spectrometry (UPLC-MS)**

UPLC-MS was performed on a Waters Xevo G2-XS, equipped with a time-of-flight mass spectrometer utilizing electrospray ionization. Samples were dissolved at 100 μM in appropriate acetonitrile/water mixtures for analysis (with 0.1% formic acid). Separation was achieved on a Waters BEH C18 column with eluent gradients of 5–80% acetonitrile in water to 100% acetonitrile over 8 minutes. Polypeptoid materials were detected by UV absorption at 214 nm. Doubly, triply, and quadruply charged species were detected, with the addition of two, three, or four ions ($H^+$ or $Na^+$), respectively.

**Gel permeation chromatography (GPC)**

Analytical chromatography was performed on a Waters e2695 GPC at 35 °C with THF as the eluent (Figure SI-3). The instrument was equipped with an Agilent 6μm MiniMIX-D column, Waters 2414 differential refractive index detector, and Waters 2998 PDA detector (monitoring at

214 nm and 254 nm). Molecular weights were calibrated using polystyrene standards in the range 350–350,000 Da.

Preparatory GPC (prep-GPC) was performed on a similar Waters system equipped with an Agilent 10μm MIXED-D column, with THF as the eluent.

**Small-angle X-ray scattering (SAXS)**

Samples were prepared by sealing one side of aluminum washers with Kapton tape, with Kapton film blocking the adhesive in the center. Dry diblock copolymer samples were added to the center and annealed at reduced pressure ($4 \times 10^{-8}$ Torr) at 170 °C for at least 3 hours, then cooled at 1 °C/min to 110 °C and annealed for at least 16 hours to form equilibrium bulk morphologies. After cooling to room temperature in vacuum, the second side of the washer was sealed.

SAXS was performed at the Advanced Light Source (ALS, beamline 7.3.3),[37] the Stanford Synchrotron Radiation Lightsource (SSRL, beamline 1-5), the National Synchrotron Light Source II (NSLS-II, beamline 11-BM), and the Advanced Photon Source (APS, beamline 12-ID-B). The beamlines were configured with X-ray energies of 10–14 keV with sample-to-detector distances of 2.8–3.6 m. Order–disorder transitions were determined at SSRL, with heating performed on a home-built stage, where temperature was measured directly at the sample position to ensure accuracy. After being loaded into the heating stage, samples were heated above 100 °C and allowed to equilibrate for 30 min before heating monotonically, equilibrating 5–15 min at each temperature before collecting exposures (Figure SI-4). Calibration using silver behenate standards, circular averaging, and correction for empty cell scattering were performed using the Nika package for Igor Pro.[38]

**Self-consistent field theory (SCFT)**

An SCFT framework was employed in which the sequence defined block copolymers are modeled as an incompressible melt of discrete Gaussian chains, with one bead of specified type for each polypeptoid residue.[39] The PS block was reduced to a discrete chain with one bead per reference volume of 0.1 $nm^3$ and elaborated to a chain of 50 beads consistent with the measured molecular weight and literature density. Periodic boundary conditions were applied, and a variable cell technique allows for cell relaxation.[40] To obtain a candidate morphology unit-cell structure, the symmetry of the corresponding space group was enforced on all fields and the simulation cell. The modified diffusion equations associated with forward and backward chain propagators were solved pseudospectrally.[41,42] Fields were relaxed to saddle-point configurations using a semi-implicit scheme.[39,43] Phase boundaries were located by comparing the intensive mean-field free energies of the candidate phases.

The three binary $\chi$ values were set in the following ratio: $\chi_{PS–Nme}$:$\chi_{PS–Npe}$:$\chi_{Nme–Npe}$ 1.0:0.8:0.2. The two polystyrene–polypeptoid $\chi$s were each measured at 220 °C via application of the random phase approximation (RPA) to SAXS curves of the disordered phase. The Nme–Npe $\chi$ was estimated based on reference 32 and by comparing SCFT predictions to experiment. Density profiles reported here are shown at $\chi_{PS–Nme}N = 25$.

RESULTS AND DISCUSSION

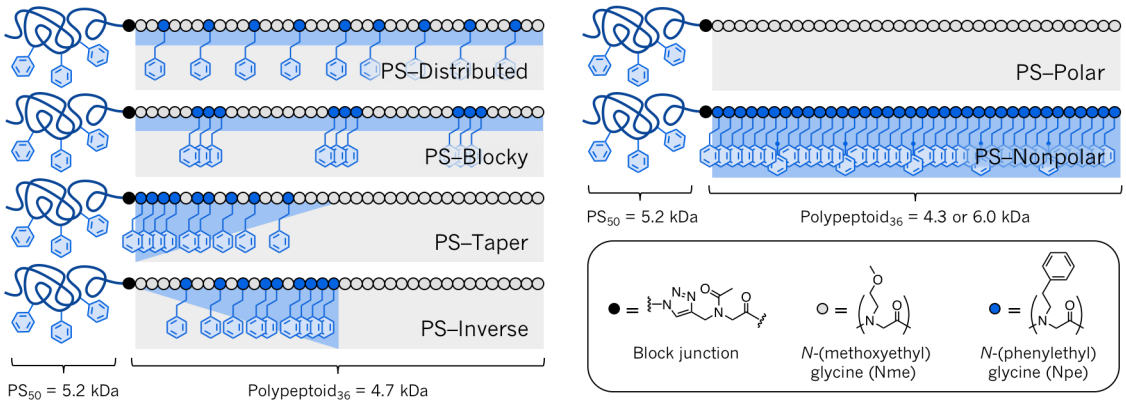


**Figure 1.** Summary of polystyrene-*b*-polypeptoid diblock copolymers. Four copolypeptoids with identical composition (left) were designed with compatibilizing groups distributed along the chain (as single units or blocks of three) or tapered from the block junction (forward or inverse). These sequences, a non-compatibilized sequence, and a fully-compatibilized sequence (right) were each clicked to polystyrene to form sequence-defined diblock copolymers.

**Synthesis of polystyrene–polypeptoid diblock copolymers**

Four polystyrene-*b*-copolypeptoid diblock copolymers were designed to share a common composition, and were expected to form ordered morphologies with accessible order–disorder transitions.[36] Two classes of sequences were synthesized, with compatibilizing groups distributed along the polypeptoid chain length (in blocks of 1 or 3) or tapered from the block junction (either forward or inverse) (Figure 1). The sequences were selected based on a fit statistic (sum of squared residuals) that was calculated against target composition profiles from all permutations of 27 and 9 beads, representing 27 polar side chains and 9 compatibilizing side chains. The composition at each unit was defined by a moving window average that sampled three repeat units to each side of the target bead, and the permutation with the lowest fit statistic was selected for each sequence (Figure SI-1).

Alkyne-terminated polypeptoids were successfully synthesized via solid phase synthesis using the submonomer method[24] and are summarized in Table 1. Two polypeptoid repeat units were chosen: a polar side chain to encourage self-assembly (*N*-(2-methoxyethyl)glycine, Nme), and another to mimic the phenyl side chains of polystyrene to tune compatibility (*N*-(2-phenylethyl)glycine, Npe). The all-polar sequence was synthesized as a homopolypeptoid of Nme. The all-nonpolar sequence was synthesized as a copolypeptoid of Npe and *N*-(2-phenylpropyl)glycine (Npp) to prevent crystallization.[29] Solid-phase polypeptoid synthesis produced the target sequences with high fidelity (Figure SI-2).

**Table 1.** Summary of polypeptoids synthesized and their characteristics

| Sequence name | Sequence | Mass (observed/ theoretical) |
|---|---|---|
| Distributed | Ac-Nprg-NmeNme(NpeNme$_3$)$_4$NpeNme$_2$(NpeNme$_3$)$_3$NpeNme$_2$ | 4712.0/4712.6 |
| Blocky | Ac-Nprg-Nme$_5$Npe$_3$Nme$_9$Npe$_3$Nme$_8$Npe$_3$Nme$_5$ | 4712.9/4712.6 |
| Taper | Ac-Nprg-Npe$_4$NmeNpe$_2$NmeNpeNmeNpeNme$_2$NpeNme$_{22}$ | 4712.1/4712.6 |
| Inverse | Ac-Nprg-Nme$_4$NpeNme$_2$NpeNmeNpeNmeNpe$_2$NmeNpe$_4$Nme$_{18}$ | 4712.1/4712.6 |
| Polar | Ac-Nprg-Nme$_{36}$ | 4298.1/4298.4 |
| Nonpolar | Ac-Nprg-Npe$_6$(NppNpe$_5$)$_5$ | 6027.3/6027.2 |

Polypeptoid sequences are written left to right from N- to C-terminus. "Ac" denotes acetylated endgroup, "Nprg" denotes *N*-(propargyl)glycine, "Nme" denotes *N*-(methoxyethyl)glycine, "Npe" denotes *N*-(phenylethyl)glycine, "Npp" denotes *N*-(phenylpropyl)glycine. The C-terminus of all polypeptoids is an amide.

Block copolymers were synthesized by conjugating alkyne-terminated polypeptoids with azide-terminated polystyrene via copper-mediated azide–alkyne click chemistry. All materials were synthesized from the same batch of azido-polystyrene, with low dispersity (Đ = 1.12). Extreme care was taken to purify diblock copolymers from unreacted homopolymer.

Precipitation followed by prep-GPC yielded isolated diblocks with effectively no homopolymer impurities, as determined by MALDI-MS (Figure 2). A summary of molecular properties is shown in Table 2.

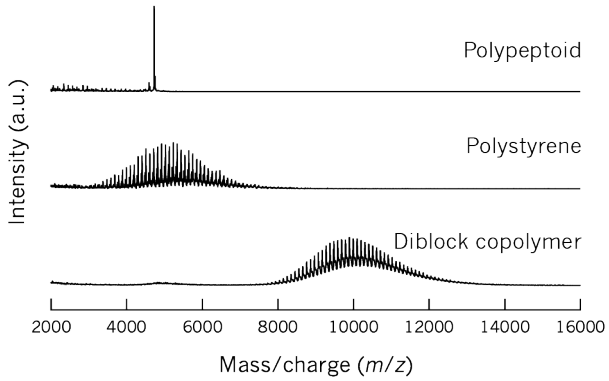


**Figure 2.** Representative MALDI mass spectrometry of the constituent blocks and diblock copolymer after purification. The material shown is PS–Distributed. Spectra are vertically offset for clarity.

**Self-assembly of polystyrene–polypeptoid diblock copolymers**

Both domain spacing and order–disorder transition temperature were found to depend on sequence, likely due to a combination of two factors: chain conformation effects arising from the localization of compatibilizing groups and tuning of the segregation strength between blocks. First, domain spacing is discussed in the context of possible preferred chain conformations. Next, order–disorder transitions are compared with effective $\chi$ parameters, calculated by applying the random phase approximation to X-ray scattering of the disordered phase, and simulations using self-consistent field theory. Overall, it is found that sequence-dependent chain conformations dominate the observed behaviors, as "smearing out" of the sequence to measure an effective $\chi$ and coarse-grained simulations both fail to capture thermodynamic transitions that arise from molecular-scale effects.

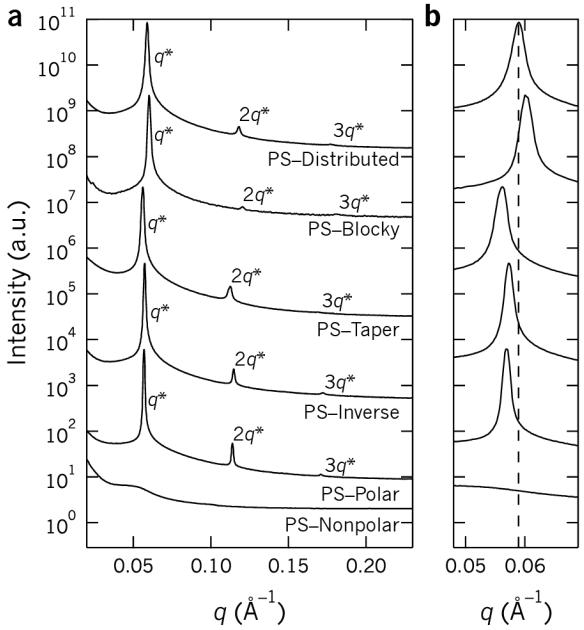


**Figure 3.** Small-angle X-ray scattering of polystyrene–polypeptoid diblock copolymers. a) Peaks at integer multiples of the primary peak ($q^*$) show that all materials form a lamellar morphology except the nonpolar block copolymer. b) Magnifying the low-$q$ region reveals differences in primary peak position. The dashed line is a guide to the eye centered at $q^*$ of PS–Distributed. Data shown were collected at room temperature and are vertically offset for clarity.

All PS–copolypeptoid diblock copolymers formed lamellar microstructures, assigned via small-angle X-ray scattering (SAXS) by the appearance of a sharp primary peak ($q^*$) and peaks at integer multiples of $q^*$ (Figure 3a). Domain spacing was calculated from the position of the primary scattering peak as $d = 2\pi/q^*$ (Figure 3b), and was found to vary significantly with sequence, despite all sequence-defined materials sharing the exact same composition and length (Figure 4a, Table 2). Simulations performed with self-consistent field theory reproduce the relative domain spacings measured by SAXS as $d_{\text{PS–Taper}} > d_{\text{PS–Inverse}} > d_{\text{PS–Distributed}} > d_{\text{PS–Blocky}}$, and the distribution of components within the lamellar domain varies as a function of sequence, as shown in simulated density profiles (Figure 4c). Notably, the compatibilizing Npe groups of PS–Taper are strongly localized at the domain interfaces, reflecting their placement in the

sequence near the block junction and their affinity for the polystyrene-rich region. The distributed sequences (PS–Distributed and PS–Blocky) have more compatibilizing groups in the center of the domain, and PS–Inverse has an intermediate profile.

**Table 2.** Self-assembly of PS–polypeptoid diblock copolymers

| Sample name | PS $M_n$ (g/mol)[a] | PS Đ[a] | Polypeptoid mass (g/mol) | $f_{peptoid}$ | Morphology | Domain spacing (± 0.03 nm) | $T_{ODT}$ (± 1 °C) |
|---|---|---|---|---|---|---|---|
| PS–Distributed | 5200 | 1.12 | 4712 | 0.44 | LAM | 10.73 nm | 143 °C |
| PS–Blocky | 5200 | 1.12 | 4712 | 0.44 | LAM | 10.29 nm | 143 °C |
| PS–Taper | 5200 | 1.12 | 4712 | 0.44 | LAM | 11.21 nm | 151 °C |
| PS–Inverse | 5200 | 1.12 | 4712 | 0.44 | LAM | 10.89 nm | 153 °C |
| PS–Polar | 5200 | 1.12 | 4298 | 0.42 | LAM | 11.06 nm | 205 °C |
| PS–Nonpolar | 5200 | 1.12 | 6027 | 0.51 | DIS | N.A. | N.A. |

"LAM" denotes lamellar, "DIS" denotes disordered. [a]PS number-average molecular weight ($M_n$) and dispersity (Đ) were determined by GPC against polystyrene standards. The volume fraction of peptoid ($f_{peptoid}$) was calculated using a polypeptoid density of 1.18 g/cm$^3$, as measured in reference 36, and polystyrene density of 1.04 g/cm$^3$. The order–disorder transition temperature ($T_{ODT}$) was determined by temperature-dependent SAXS.

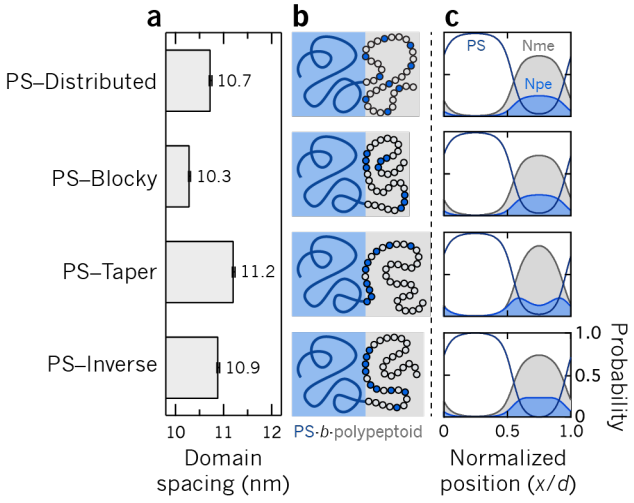

**Figure 4.** a) Domain spacing of lamellar sequence-defined diblock copolymers as measured by SAXS. Error bars arise from limited instrument resolution in $q$ and residuals to fits to the primary scattering peak by a Gaussian function. b) Schematics of representative chain conformations that result in the measured domain spacings. Polypeptoid sequences with compatibilizing groups distributed along the length of the block have smaller domain spacings compared to sequences with long polar tails, likely due to promoted insertion into the PS microdomain. c) Density profiles for components within the lamellar domain as predicted by SCFT.

The variation in domain spacing can be rationalized with an enthalpic argument, where the system's energy is lowered by adopting chain conformations that minimize the enthalpy of mixing (Figure 4b). The system suffers an energetic penalty when polar and nonpolar side chains are forced to mix, but this unfavorable interaction can be avoided by inserting the nonpolar components of the polypeptoid into the polystyrene microdomain. This enthalpic effect alters the chain conformation in both the ordered and disordered phases, as evidenced by domain spacing and disordered phase radius of gyration that both track with sequence (Figure 5). However, the relative variation in $R_g$ is smaller than that measured in domain spacing (plotted on proportional axes, the dashed lines in Figure 5 demonstrate the total variation in domain spacing with sequence; the variation in $R_g$ is much within these bounds). Since it is expected that $d \sim R_g$, the conformational effects stemming from the sequence of compatibilizing groups must be exaggerated in the ordered phase—where all of the nonpolar polypeptoid units have mainly polar polypeptoid as nearest neighbors, as opposed to the prevalence of nearby nonpolar polystyrene in the disordered phase.

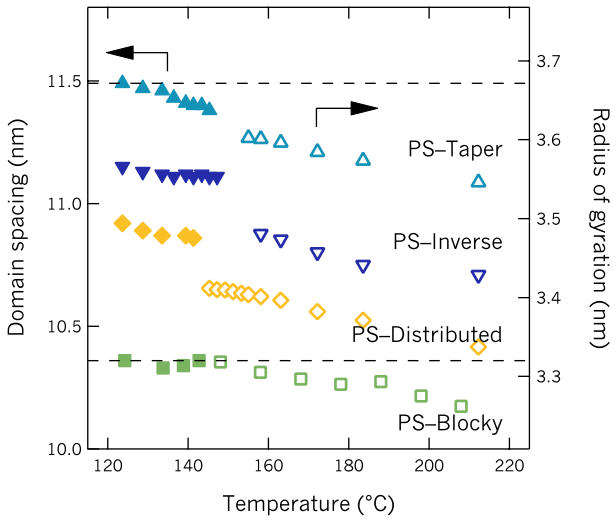


**Figure 5**. Characteristic lengthscales as a function of temperature and sequence. Domain spacing (left axis, closed symbols) was calculated using the primary scattering peak in the ordered state ($d = 2\pi/q^*$), and radius of gyration (right axis, open symbols) was taken from RPA fits in the disordered state. Values are plotted on proportional axes, and dashed lines indicate the total variation in domain spacing at 125 °C. All error bars are smaller than the markers.

The sequences with the smallest domain spacings are PS–Blocky and PS–Distributed (10.29 nm and 10.73 nm, respectively). All domain spacings have an error of ± 0.03 nm. These sequences have compatibilizing phenyl units distributed along the entire block length, which likely promotes flattened chain conformations that allow these nonpolar units to access the PS–polypeptoid interface more easily and lead to a smaller domain spacing. This hypothesis is supported by simulations performed with SCFT. Key regions of the polypeptoid block were selected as tracers (the chain middle and chain end, Figure 6a), and an example density profile for these tracers in the ordered lamellar phase is shown in Figure 6b, with probability (normalized by the maximum probability) plotted against position within the lamellar

microdomain (normalized by domain spacing). For the sequences with distributed compatibilizing groups (PS–Distributed and PS–Blocky), the polypeptoid chain end is more likely to be at the PS–polypeptoid interface than for the tapered sequences or polar sequence (Figure 6d), which causes these materials to have more compact chain conformations and smaller domain spacings.

Conversely, the tapered sequence (PS–Taper) has the largest domain spacing (11.21 nm). With all of its compatibilizing groups placed near the block junction, a long polar tail is left to extend into and expand the domain. The inverse taper sequence (PS–Inverse) has elements of both these extremes and, as expected, an intermediate domain spacing (10.89 nm). Its compatibilizing units are concentrated toward the center of the block, allowing the middle of the polypeptoid chain to localize at the PS interface and fold the chain into a more compact conformation. However, the lack of nonpolar units in the second half of the sequence may cause PS–Inverse to take on conformations that are more extended than the distributed sequences, whose chain ends have nonpolar units that can localize at the interface and thus shrink the domain. In Figure 6c, we see from simulations that, indeed, the middle of the Taper block is more likely to lie in the center of the polypeptoid domain than the middle of the Inverse block, whose nonpolar units are seen to migrate more strongly toward the interface. Further, the polar chain ends of both the Taper and Inverse blocks are much more likely to be in the polypeptoid microdomain center than either of the distributed sequences (Figure 6d).

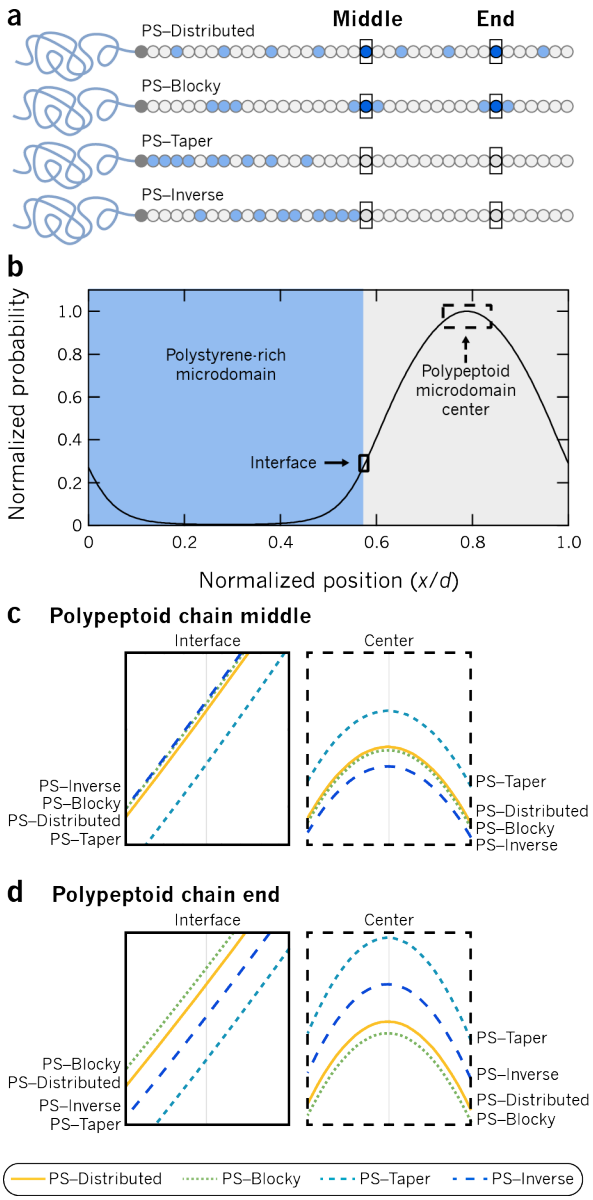


**Figure 6.** Composition profiles predicted by SCFT simulations. a) Two regions of the polypeptoid chain were chosen as tracers: the middle and near the chain end. b) A representative density profile is plotted against position within the lamellar microdomain, with the PS-rich region depicted on the left and polypeptoid-rich region on the right. Insets of the domain interface and polypeptoid domain center are shown for the c) middle region and d) chain end tracers. Comparing density profiles between sequences supports the existence of chain conformational effects in the ordered phase.

Comparing the two distributed sequences, PS–Blocky has a smaller domain spacing than PS–Distributed. The effect of "blockiness" in copolymers, or the presence of consecutive repeats of the same monomer, has been well-documented to affect phase behavior, surface adsorption, and globule formation, with the common effect of increasing the driving force for similar functional groups to cluster together.[13,44-47] Here, we see that a blocky-distributed sequence, with phenyl units arranged in blocks of three, shrinks the domain spacing as compared to the distributed sequence with single isolated units. The blockiness exaggerates chain compaction due to a stronger driving force for blocky compatibilizing groups to leave the polar polypeptoid region and move to the interface with polystyrene. This is supported by simulation, where the chain-end of the Blocky sequence is more likely to be found at the interface than that of the Distributed sequence (and less likely to be found in the polypeptoid domain center, Figure 6d). While we compare just two materials here, there is an opportunity to further study the effects of blockiness using polypeptoids as a model system.

The all-polar diblock copolymer (PS–Polar) also forms a lamellar morphology and serves as a benchmark for a completely non-compatibilized system. With no bulky aromatic units, PS–Polar has a smaller chain volume than any of the sequence-defined copolymers, but its domain spacing is intermediate (11.06 nm ± 0.03 nm), not the smallest as might be expected. This is a result of the relatively high $\chi$ of the fully polar diblock copolymer, which leads to increased chain stretching and expanded domains, along with a low likelihood to adopt compacted chain conformations available to sequences with compatibilizing groups that can insert into the polystyrene domain. The combination of a smaller chain volume with the expanding property of a higher $\chi$ is reflected in an intermediate domain spacing.

The all-nonpolar diblock copolymer (PS–Nonpolar) was found to be disordered (Figure 3). This material was designed to have the lowest $\chi$ and demonstrates the successful use of phenyl side chains to compatibilize the polar polypeptoid backbone to polystyrene.

Through enthalpic arguments and corresponding simulations, it is clear that there are sequence-dependent chain conformational effects within the polypeptoid-rich region in the ordered phase, resulting in expanded or contracted domains. We next quantitatively measure the effect of sequence on the effective interaction parameter $\chi_{\text{eff}}$, as deduced from the structure factor of the disordered phase, and compare geometric observations with the effects of changing segregation strength.

**Role of sequence in segregation strength**

Adding compatibilizing phenyl groups lowers the interaction parameter between the polar polypeptoid and nonpolar polystyrene blocks, with the precise sequence in which compatibilizing groups are incorporated resulting in variations in the order–disorder transition temperature and effective $\chi$, despite the different copolypeptoid materials having the same composition. In addition to the geometric differences discussed above, these thermodynamic differences suggest that the details of monomer-level sequence are critical in dictating the segregation strength.

To quantify the segregation strength between blocks, we applied the random phase approximation (RPA) for a diblock copolymer melt to scattering profiles in the disordered phase,[1] extracting an effective $\chi$ parameter ($\chi_{\text{eff}}$) as a function of sequence and temperature (see SI for fit details). We use the term "effective" interaction parameter to refer to a simple PS–polypeptoid $\chi$, where the polypeptoid is considered to be a homogeneous or "smeared out" block

for the purpose of fitting to the diblock copolymer RPA expression. This approach was favored over other treatments, such as comparing the order–disorder transition to mean field theory predictions, due to suspected non-ideal chain conformations.

The disordered phase is accessible for all materials upon heating, as evidenced by the transition to a broad scattering peak corresponding to density fluctuations in the disordered melt that arise from the connectivity of the two dissimilar blocks. The $q$-position of the peak corresponds to the lengthscale of fluctuations (determined by the radius of gyration, $R_g$, of the block copolymer), and the breadth of the peak is determined by the strength of the interaction parameter. Due to a combination of unfavorable chain stretching at long lengthscales and dominant intrablock correlations at monomer lengthscales, the structure factor approaches zero intensity at both low- and high-$q$ limits, respectively. Scattering curves were fit well with RPA (Figure 7) using $\chi_{eff}$, $R_g$, and $C$ as adjustable parameters, where $C$ is a scaling constant that accounts for the arbitrary units of intensity and for constant prefactors related to scattering contrast and volume. It was assumed that the diblock copolymers were conformationally symmetric (statistical segment lengths for polystyrene and polypeptoids are similar, at 0.5 nm[48] and 0.4 nm[49], respectively). A reference volume of 0.1 $nm^3$ was used.

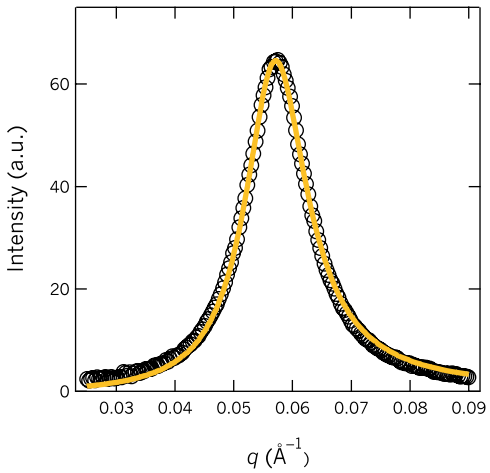


**Figure 7.** Representative SAXS profile in the disordered phase, fit with the random phase approximation allowing effective interaction parameter ($\chi_{eff}$), radius of gyration ($R_g$), and a scaling constant $C$ to vary. Data are shown with black circles; the fit is shown with a yellow line. The example shown is PS–Distributed at 147 °C.

As expected, PS–Polar, with no compatibilizing groups, has the highest interaction parameter (Figure 8a). All sequence-defined diblock copolymers have lower $\chi_{eff}$ values, indicating that the incorporation of compatibilizing phenyl groups directly lowers the effective interaction parameter. Compatibilization is also evidenced by differences in order–disorder transition temperatures (Figure 8b). PS–Polar has the highest $T_{ODT}$ at 205 °C, corroborating the high $\chi$ parameter measured between the polar polypeptoid and nonpolar polystyrene, especially given the small total molecular weight of ~10 kDa. By replacing 25% of the polar ether side chains with nonpolar phenyl groups, the $T_{ODT}$ drops by as much as 62 °C, demonstrating a lowered interaction parameter with the polystyrene block.

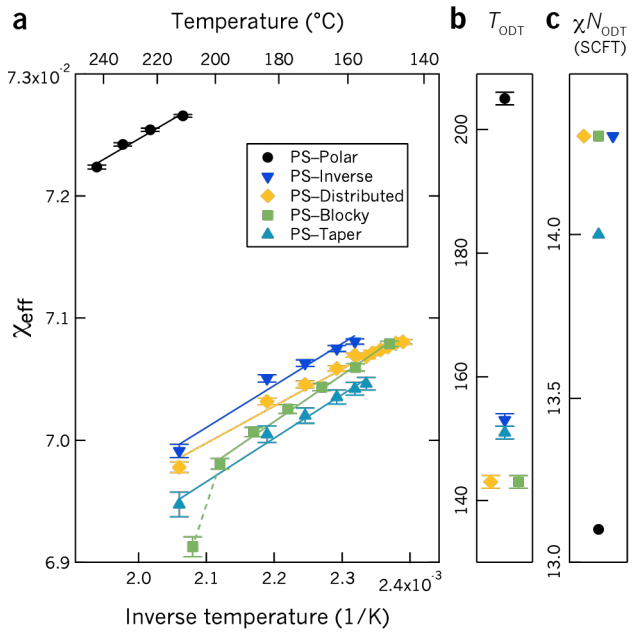


**Figure 8.** a) The PS–polypeptoid effective interaction parameter ($\chi_{eff}$) varies as a function of sequence and temperature. Effective $\chi$s were measured by applying the random phase approximation to scattering curves of the disordered phase (reference volume $v_0$ = 0.1 nm$^3$). Solid lines are fits with the relationship $\chi_{eff} = A/T + B$, and error bars represent 95% confidence intervals from the fits. The dashed line is a guide to the eye and may signify a second order dependence on inverse temperature, possibly due to the breaking up of nonpolar aggregates of Npe side chains. b) Order–disorder transition temperature and c) $\chi N$ at the ODT (as predicted by SCFT) both vary with sequence. Neither $\chi_{eff}$ nor $\chi N_{ODT}$ reproduce the trends seen in the experimental $T_{ODT}$.

Among the sequence-defined copolypeptoid diblocks, the $T_{ODT}$ varies markedly as a function of sequence. The diblock copolymers with distributed sequences (PS–Distributed and PS–Blocky) disorder at the lowest temperature, both at 143 °C (± 1 °C for all $T_{ODT}$s). With compatibilizing groups distributed along the chain length, the nonpolar repeat units may be better solubilized in the polar polypeptoid, resulting in mixing (disordering) at lower temperatures upon

heating. PS–Taper disorders at an intermediate temperature (151 °C), and PS–Inverse disorders at the highest temperature (153 °C). Comparing to references 8 and 9, the observed reversal of the relative transition temperatures between tapered and inverse tapered materials is likely due to a combination of two major differences between the systems: precise (versus average) sequence control and the use of a "styrene-like" compatibilizing group in this system. Dispersity in comonomer sequence is expected to affect relative phase stability, and the use of a "styrene-like" side chain leads to a weaker compatibilization between the two blocks compared to a system that incorporates pure styrene repeat units into the polypeptoid block (which is impossible to do with the present chemistry).

Within the compatibilized materials, it is informative to compare the calculated $\chi_{\text{eff}}$ parameters with the measured order–disorder transition temperatures (Figure 8a and 8b), which might be expected to track together. First, the diblock copolymer with an inverse taper has the highest $\chi_{\text{eff}}$, which is consistent with the result that it also disorders at the highest temperature. Apart from this material, the rest of the effective interaction parameters do not match their order–disorder transition temperatures: the tapered sequence has the lowest $\chi_{\text{eff}}$, although it has the second highest disordering temperature, and the distributed sequences have intermediate $\chi_{\text{eff}}$s but share the lowest disordering temperature. With this disagreement, it is important to consider that the order–disorder transition is inherently tied to both the ordered and disordered phases, because it corresponds to a point where their free energies coincide. Here, $\chi_{\text{eff}}$ is measured only in the disordered phase, and with sequence-dependent conformations in the ordered phase, this $\chi_{\text{eff}}$ does not necessarily describe the ordered phase or the transition to disorder. The lack of agreement between measured phase transitions and the relative order of effective $\chi$ parameters emphasizes the need for molecular-lengthscale information in applying RPA analyses to

copolymer systems with varying distributions of comonomers. For example, this work implies that the application of a single $\chi$ parameter to a random copolymer may not fully capture the details of monomer-lengthscale distribution of functional groups, especially at short polymer lengths.

Further, if the effective $\chi$ concept were valid for these sequence-defined materials, then the domain spacing $d$ in the lamellar phase could be related to $\chi_{eff}$ by a form imposed by SCFT: $d = R_g F(\chi_{eff}N)$, where $R_g$ is the disordered phase radius of gyration and $F$ is a dimensionless function of $\chi_{eff}N$. From the RPA fits above the order–disorder transition, we find that the order of $R_g$ parallels that of $d$ (Figure 6), satisfying $d \sim R_g$ and indicating that some degree of the conformational effects detected in the ordered phase persist into the disordered phase. The function $F$ is known numerically to be approximately 3.2 near the ODT at $\chi_{eff}N \sim 10$, and asymptotically scales as $(\chi_{eff}N)^{1/6}$ for strong segregation strength.[50] Furthermore, $F$ is a monotonically increasing function of $\chi_{eff}N$, so a sequence-specific trend in $\chi_{eff}$ must translate into the same trend in $d$ if the effective $\chi$ concept were to hold. Since this is not observed, we conclude that the notion of replacing a heterogeneous block by a "smeared out" homogenous block with an effective interaction parameter is too simplistic and has little predictive value for order–disorder transitions or ordered phase properties. Indeed, even for block polymers with purely homogeneous blocks, $T_{ODT}$ and $d$ are sensitive to block architecture and molecular weight, reflecting a complex balance of enthalpic interactions and conformational entropy in the ordered state.[51] It is therefore unreasonable to expect that sequence-dependent effects in polymers with heterogeneous blocks could be predicted by an effective $\chi$ deduced from the disordered state, and more complex descriptors that account for chain conformational effects should be pursued.

Finally, order–disorder transitions were calculated by SCFT simulations (Figure 8c) by comparing the intensive mean-field free energies of the candidate phases, employing the same three-$\chi$ framework and full sequence definition utilized in calculating the relative domain spacings above. A large difference is correctly predicted between PS–Polar and the rest of the materials, but the trends within the sequence-defined materials do not agree with those measured in experiment. While SCFT (mean-field theory) captures structural effects in the ordered phase well, such as the geometric effects seen in domain spacing and chain conformations, the location of the phase transition is sensitive to fluctuation effects in both disordered and ordered phases, so it is not surprising that the sequence-dependent trends in the order–disorder transition are not reproduced. This is further evidence that more complex approaches that explicitly account for chain conformation should be pursued to describe systems with heterogeneous blocks.

## CONCLUSIONS

A series of sequence-defined diblock copolymers was synthesized, and both morphological and thermodynamic effects were measured. It was found that domain spacing and order–disorder transition temperature are functions of sequence. The differences in these parameters are attributed to the dominating effect of an altered chain conformation in the ordered state that localizes compatibilizing groups at the polystyrene–polypeptoid interface.

Sequences with distributed compatibilizing groups have smaller domain spacings and lower order–disorder transition temperatures than those with compatibilizing groups tapered from the block junction (either forward or inverse). Simulations using self-consistent field theory reproduce the relative domain spacings and predict different distributions of compatibilizing groups within the polypeptoid domain based on sequence, supporting the suggested

conformational effects in the ordered state. In the disordered state, altered chain conformations persist, as evidenced by relative radii of gyration that parallel the relative domain spacings. However, the mismatch between sequence-specific trends in order–disorder transition temperatures and effective interaction parameters (extracted from disordered phase scattering measurements) suggests that the effective $\chi$ concept has limited predictive value in anticipating $T_{ODT}$ or ordered phase properties of sequence-specific block copolymers. Similarly, simulations performed with SCFT also do not match the trends seen in $T_{ODT}$, further demonstrating that these coarse-grained approaches do not capture thermodynamic trends seen in sequence-defined materials.

These results suggest that monomer-level sequence control influences both morphological and thermal properties via chain conformational effects. Exercising such sequence control could lead to new materials with tunable self-assembly properties based on sequence alone.

## ASSOCIATED CONTENT

### Supporting information

Sequence design, polypeptoid analytical UPLC traces, polystyrene GPC, order–disorder transition plots, and details on the random phase approximation.

## AUTHOR INFORMATION


### Corresponding Author

*E-mail: segalman@engineering.ucsb.edu

### Present Addresses

[§]E.C.D.: John A. Paulson School of Engineering and Applied Sciences, Wyss Institute for Biologically Inspired Engineering, Harvard University, Cambridge, MA 02138

**Author Contributions**

The manuscript was written through contributions of all authors. All authors have given approval to the final version of the manuscript.

ACKNOWLEDGMENTS

The authors gratefully acknowledge funding from the National Science Foundation (NSF) Division of Materials Research (DMR) Polymers program (DMR-1608297) for synthesis and characterization of block copolymers and the NSF Condensed Matter and Materials Theory Program (DMR-1822215) for the SCFT simulations. A.L.P. gratefully acknowledges the NSF for a graduate research fellowship. Polypeptoid characterization and block copolymer purification were performed with guidance from Dr. Rachel Behrens and with support from the MRL Shared Experimental Facilities (supported by the MRSEC Program of the NSF, DMF-1720256; a member of the NSF-funded Materials Research Facilities Network). SCFT simulations utilized resources of the Center for Scientific Computing from the UCSB CNSI, MRL, and NSF MRSEC (DMR-1720256) and NSF CNS-1725797. X-ray scattering experiments utilized resources of the Advanced Light Source (a U.S. Department of Energy (DOE) Office of Science User Facility, DE-AC02-05CH11231; beamline 7.3.3), the Stanford Synchrotron Radiation Lightsource (supported by the U.S. DOE Office of Science, Office of Basic Energy Sciences, DE-AC02-76SF00515; beamline 1-5), the National Synchrotron Light Source II (a U.S. DOE Office of Science User Facility operated for the DOE Office of Science by Brookhaven National Laboratory, DE-SC0012704; beamline 11-BM), and the Advanced Photon

Source (a U.S. DOE Office of Science User Facility operated for the DOE Office of Science by Argonne National Laboratory, DE-AC02-06CH11357). A.L.P. thanks Dr. Morgan Schulze (UCSB) for X-ray scattering resources and Andrew Turner (MIT) for input in programming the sequence selection. The authors also thank Dr. Ron Zuckermann at the Molecular Foundry of the Lawrence Berkeley National Lab for helpful discussions regarding polypeptoid synthesis.

REFERENCES

(1) Leibler, L. Theory of Microphase Separation in Block Copolymers. *Macromolecules* **1980,** *13* (6), 1602-1617.
(2) Beckingham, B. S.; Register, R. A. Synthesis and Phase Behavior of Block-Random Copolymers of Styrene and Hydrogenated Isoprene. *Macromolecules* **2011,** *44* (11), 4313-4319.
(3) Quinn, J. D.; Register, R. A. Microphase Separation in Block-Random Copolymers of Styrene, 4-Acetoxystyrene, and 4-Hydroxystyrene. *J. Polym. Sci. Pol. Phys.* **2009,** *47* (21), 2106-2113.
(4) Kim, J.; Gray, M. K.; Zhou, H. Y.; Nguyen, S. T.; Torkelson, J. M. Polymer Blend Compatibilization by Gradient Copolymer Addition During Melt Processing: Stabilization of Dispersed Phase to Static Coarsening. *Macromolecules* **2005,** *38* (4), 1037-1040.
(5) Wong, C. L. H.; Kim, J.; Torkelson, J. M. Breadth of Glass Transition Temperature in Styrene/Acrylic Acid Block, Random, and Gradient Copolymers: Unusual Sequence Distribution Effects. *J. Polym. Sci. Pol. Phys.* **2007,** *45* (20), 2842-2849.
(6) Jouenne, S.; Gonzalez-Leon, J. A.; Ruzette, A.-V.; Lodefier, P.; Tence-Girault, S.; Leibler, L. Styrene/Butadiene Gradient Block Copolymers: Molecular and Mesoscopic Structures. *Macromolecules* **2007,** *40* (7), 2432-2442.
(7) Mastroianni, S. E.; Epps, T. H., III Interfacial Manipulations: Controlling Nanoscale Assembly in Bulk, Thin Film, and Solution Block Copolymer Systems. *Langmuir* **2013,** *29* (12), 3864-3878.
(8) Singh, N.; Tureau, M. S.; Epps, T. H., III Manipulating Ordering Transitions in Interfacially Modified Block Copolymers. *Soft Matter* **2009,** *5* (23), 4757-4762.
(9) Roy, R.; Park, J. K.; Young, W. S.; Mastroianni, S. E.; Tureau, M. S.; Epps, T. H., III Double-Gyroid Network Morphology in Tapered Diblock Copolymers. *Macromolecules* **2011,** *44* (10), 3910-3915.
(10) Tsukahara, Y.; Nakamura, N.; Hashimoto, T.; Kawai, H.; Nagaya, T.; Sugimura, Y.; Tsuge, S. Structure and Properties of Tapered Block Polymers of Styrene and Isoprene. *Polym. J.* **1980,** *12* (7), 455-466.

(11) Lutz, J. F.; Schmidt, B. V. K. J.; Pfeifer, S. Tailored Polymer Microstructures Prepared by Atom Transfer Radical Copolymerization of Styrene and N-Substituted Maleimides. *Macromol. Rapid Commun.* **2011,** *32* (2), 127-135.
(12) Seo, Y.; Brown, J. R.; Hall, L. M. Effect of Tapering on Morphology and Interfacial Behavior of Diblock Copolymers from Molecular Dynamics Simulations. *Macromolecules* **2015,** *48* (14), 4974-4982.
(13) Ganesan, V.; Kumar, N. A.; Pryamitsyn, V. Blockiness and Sequence Polydispersity Effects on the Phase Behavior and Interfacial Properties of Gradient Copolymers. *Macromolecules* **2012,** *45* (15), 6281-6297.
(14) Chang, L. W.; Lytle, T. K.; Radhakrishna, M.; Madinya, J. J.; Velez, J.; Sing, C. E.; Perry, S. L. Sequence and Entropy-Based Control of Complex Coacervates. *Nat. Commun.* **2017,** *8*.
(15) Barnes, J. C.; Ehrlich, D. J. C.; Gao, A. X.; Leibfarth, F. A.; Jiang, Y. V.; Zhou, E.; Jamison, T. F.; Johnson, J. A. Iterative Exponential Growth of Stereo- and Sequence-Controlled Polymers. *Nat. Chem.* **2015,** *7* (10), 810-815.
(16) Jiang, Y.; Golder, M. R.; Nguyen, H. V. T.; Wang, Y. F.; Zhong, M. J.; Barnes, J. C.; Ehrlich, D. J. C.; Johnson, J. A. Iterative Exponential Growth Synthesis and Assembly of Uniform Diblock Copolymers. *J. Am. Chem. Soc.* **2016,** *138* (30), 9369-9372.
(17) Gutekunst, W. R.; Hawker, C. J. A General Approach to Sequence-Controlled Polymers Using Macrocyclic Ring Opening Metathesis Polymerization. *J. Am. Chem. Soc.* **2015,** *137* (25), 8038-8041.
(18) Fu, C. K.; Huang, Z. X.; Hawker, C. J.; Moad, G.; Xu, J. T.; Boyer, C. Raft-Mediated, Visible Light-Initiated Single Unit Monomer Insertion and Its Application in the Synthesis of Sequence-Defined Polymers. *Polym. Chem.* **2017,** *8* (32), 4637-4643.
(19) Solleder, S. C.; Meier, M. A. R. Sequence Control in Polymer Chemistry through the Passerini Three-Component Reaction. *Angew. Chem., Int. Ed.* **2014,** *53* (3), 711-714.
(20) Berthet, M. A.; Zarafshani, Z.; Pfeifer, S.; Lutz, J. F. Facile Synthesis of Functional Periodic Copolymers: A Step toward Polymer-Based Molecular Arrays. *Macromolecules* **2010,** *43* (1), 44-50.
(21) Al Ouahabi, A.; Kotera, M.; Charles, L.; Lutz, J. F. Synthesis of Monodisperse Sequence-Coded Polymers with Chain Lengths above Dp100. *ACS Macro Lett.* **2015,** *4* (10), 1077-1080.
(22) Boz, E.; Wagener, K. B.; Ghosal, A.; Fu, R. Q.; Alamo, R. G. Synthesis and Crystallization of Precision Admet Polyolefins Containing Halogens. *Macromolecules* **2006,** *39* (13), 4437-4447.
(23) Baughman, T. W.; Chan, C. D.; Winey, K. I.; Wagener, K. B. Synthesis and Morphology of Well-Defined Poly(Ethylene-Co-Acrylic Acid) Copolymers. *Macromolecules* **2007,** *40* (18), 6564-6571.
(24) Zuckermann, R. N.; Kerr, J. M.; Kent, S. B. H.; Moos, W. H. Efficient Method for the Preparation of Peptoids [Oligo(N-Substituted Glycines)] by Submonomer Solid-Phase Synthesis. *J. Am. Chem. Soc.* **1992,** *114* (26), 10646-10647.
(25) Nam, K. T.; Shelby, S. A.; Choi, P. H.; Marciel, A. B.; Chen, R.; Tan, L.; Chu, T. K.; Mesch, R. A.; Lee, B. C.; Connolly, M. D.; Kisielowski, C.; Zuckermann, R. N. Free-Floating Ultrathin Two-Dimensional Crystals from Sequence-Specific Peptoid Polymers. *Nat. Mater.* **2010,** *9* (5), 454-460.

(26) Murnen, H. K.; Rosales, A. M.; Jaworsk, J. N.; Segalman, R. A.; Zuckermann, R. N. Hierarchical Self-Assembly of a Biomimetic Diblock Copolypeptoid into Homochiral Superhelices. *J. Am. Chem. Soc.* **2010,** *132* (45), 16112-16119.
(27) Armand, P.; Kirshenbaum, K.; Falicov, A.; Dunbrack, R. L.; Dill, K. A.; Zuckermann, R. N.; Cohen, F. E. Chiral N-Substituted Glycines Can Form Stable Helical Conformations. *Folding Des.* **1997,** *2* (6), 369-375.
(28) Gorske, B. C.; Mumford, E. M.; Gerrity, C. G.; Ko, I. A Peptoid Square Helix Via Synergistic Control of Backbone Dihedral Angles. *J. Am. Chem. Soc.* **2017,** *139* (24), 8070-8073.
(29) Rosales, A. M.; Murnen, H. K.; Zuckermann, R. N.; Segalman, R. A. Control of Crystallization and Melting Behavior in Sequence Specific Polypeptoids. *Macromolecules* **2010,** *43* (13), 5627-5636.
(30) Greer, D. R.; Stolberg, M. A.; Kundu, J.; Spencer, R. K.; Pascal, T.; Prendergast, D.; Balsara, N. P.; Zuckermann, R. N. Universal Relationship between Molecular Structure and Crystal Structure in Peptoid Polymers and Prevalence of the Cis Backbone Conformation. *J. Am. Chem. Soc.* **2018,** *140* (2), 827-833.
(31) Rosales, A. M.; Segalman, R. A.; Zuckermann, R. N. Polypeptoids: A Model System to Study the Effect of Monomer Sequence on Polymer Properties and Self-Assembly. *Soft Matter* **2013,** *9* (35), 8400-8414.
(32) Sun, J.; Teran, A. A.; Liao, X. X.; Balsara, N. P.; Zuckermann, R. N. Nanoscale Phase Separation in Sequence-Defined Peptoid Diblock Copolymers. *J. Am. Chem. Soc.* **2013,** *135* (38), 14119-14124.
(33) Sun, J.; Teran, A. A.; Liao, X. X.; Balsara, N. P.; Zuckermann, R. N. Crystallization in Sequence-Defined Peptoid Diblock Copolymers Induced by Microphase Separation. *J. Am. Chem. Soc.* **2014,** *136* (5), 2070-2077.
(34) Sun, J.; Liao, X. X.; Minor, A. M.; Balsara, N. P.; Zuckermann, R. N. Morphology–Conductivity Relationship in Crystalline and Amorphous Sequence-Defined Peptoid Block Copolymer Electrolytes. *J. Am. Chem. Soc.* **2014,** *136* (42), 14990-14997.
(35) Sun, J.; Jiang, X.; Siegmund, A.; Connolly, M. D.; Downing, K. H.; Balsara, N. P.; Zuckermann, R. N. Morphology and Proton Transport in Humidified Phosphonated Peptoid Block Copolymers. *Macromolecules* **2016,** *49* (8), 3083-3090.
(36) Rosales, A. M.; McCulloch, B. L.; Zuckermann, R. N.; Segalman, R. A. Tunable Phase Behavior of Polystyrene–Polypeptoid Block Copolymers. *Macromolecules* **2012,** *45* (15), 6027-6035.
(37) Hexemer, A.; Bras, W.; Glossinger, J.; Schaible, E.; Gann, E.; Kirian, R.; MacDowell, A.; Church, M.; Rude, B.; Padmore, H. A Saxs/Waxs/Gisaxs Beamline with Multilayer Monochromator. *J. Phys.: Conf. Ser.* **2010,** *247*.
(38) Ilavsky, J. Nika: Software for Two-Dimensional Data Reduction. *J. Appl. Crystallogr.* **2012,** *45*, 324-328.
(39) Fredrickson, G. H., *The Equilibrium Theory of Inhomogeneous Polymers*. Oxford Science Publications: Oxford, UK, 2006.
(40) Barrat, J. L.; Fredrickson, G. H.; Sides, S. W. Introducing Variable Cell Shape Methods in Field Theory Simulations of Polymers. *J. Phys. Chem. B* **2005,** *109* (14), 6694-6700.
(41) Rasmussen, K. O.; Kalosakas, G. Improved Numerical Algorithm for Exploring Block Copolymer Mesophases. *J. Polym. Sci. Pol. Phys.* **2002,** *40* (16), 1777-1783.

(42) Tzeremes, G.; Rasmussen, K. O.; Lookman, T.; Saxena, A. Efficient Computation of the Structural Phase Behavior of Block Copolymers. *Phys. Rev. E* **2002,** *65* (4), 041806-(1-5).
(43) Ceniceros, H. D.; Fredrickson, G. H. Numerical Solution of Polymer Self-Consistent Field Theory. *Multiscale Model Simul.* **2004,** *2* (3), 452-474.
(44) Jhon, Y. K.; Semler, J. J.; Genzer, J.; Beevers, M.; Gus'kova, O. A.; Khalatur, P. G.; Khokhlov, A. R. Effect of Comonomer Sequence Distribution on the Adsorption of Random Copolymers onto Impenetrable Flat Surfaces. *Macromolecules* **2009,** *42* (7), 2843-2853.
(45) Khokhlov, A. R., *Conformation-Dependent Design of Sequences in Copolymers*. Springer: Berlin ; New York, 2006.
(46) Murnen, H. K.; Khokhlov, A. R.; Khalatur, P. G.; Segalman, R. A.; Zuckermann, R. N. Impact of Hydrophobic Sequence Patterning on the Coil-to-Globule Transition of Protein-Like Polymers. *Macromolecules* **2012,** *45* (12), 5229-5236.
(47) Govorun, E. N.; Khokhlov, A. R.; Semenov, A. N. Stability of Dense Hydrophobic–Polar Copolymer Globules: Regular, Random and Designed Sequences. *Eur. Phys. J. E* **2003,** *12* (2), 255-264.
(48) Chain Dimensions and Entanglement Spacings. In *Physical Properties of Polymers Handbook*, Mark, J. E., Ed. AIP Press: Woodbury, NY, 1996.
(49) Rosales, A. M.; Murnen, H. K.; Kline, S. R.; Zuckermann, R. N.; Segalman, R. A. Determination of the Persistence Length of Helical and Non-Helical Polypeptoids in Solution. *Soft Matter* **2012,** *8* (13), 3673-3680.
(50) Matsen, M. W.; Bates, F. S. Unifying Weak- and Strong-Segregation Block Copolymer Theories. *Macromolecules* **1996,** *29* (4), 1091-1098.
(51) Matsen, M. W. Effect of Architecture on the Phase Behavior of Ab-Type Block Copolymer Melts. *Macromolecules* **2012,** *45* (4), 2161-2165.